Talbot-Lau grating interferometer XCT for the quantitative characterization of damage in polymers after impact and static tensile testing

Sascha SENCK [1], Dietmar SALABERGER [1], Christian GUSENBAUER [1], Bernhard PLANK [1], Guruprasad RAO [1], Johann KASTNER [1]
[1] University of Applied Sciences Upper Austria, Wels, Austria

Contact e-mail: sascha.senck@fh-wels.at

Abstract. X-ray imaging methods such as micro-computed tomography (XCT) are essential techniques to reveal and quantify internal defects in materials, particularly in polymers and composites. Conventional absorption-based contrast (AC) provides information on the attenuation of the X-ray beam intensity and is an invaluable tool in various domains, e.g. medicine and materials science. In the last decade however an important innovation in X-ray technology has emerged by the introduction of Talbot-Lau grating interferometer XCT. This method provides three complementary characteristics in a single scan of the specimen: a) the attenuation contrast, b) the differential phase contrast (DPC), and c) the dark-field contrast (DFC). DPC is related to the index of refraction and DFC reflects the total amount of radiation scattered at small angles, e.g. caused by microscopic inhomogeneities represented by cracks and pores.

Using a novel Talbot-Lau grating interferometer XCT system (TLGI-XCT) for laboratory applications we visualize crack-like defects in carbon fiber reinforced laminates that were subjected to impact forces up to 20 Joules. Using DFC we were able to detect cracks in samples that were subject to low impact forces whereas these defects are merely detectable using AC. Specimens were scanned at isometric voxel sizes between 5.7 and 22.8 µm. TLGI-XCT results are compared to ultrasonic examinations. Secondly, we investigate polypropylene test specimens that were cyclically loaded in tensile testing experiments until final failure. Lower grey levels near the fracture surface in the AC and DPC images indicate pores. Due to increased scattering in these regions DFC images provide a high signal intensity even though the defects are smaller than the spatial resolution. For all samples high-resolution reference measurements were carried out using an industrial XCT system.

Due to the fact that DFC delivers morphological information in the sub-pixel regime depending on the local scattering power, dark field imaging delivers information that may otherwise be inaccessible using conventional XCT. Using a Talbot-Lau XCT we show that dark field images yield a high contrast and a strong signal at interfaces, e.g. for cracks and pores.

1. Introduction

X-ray imaging methods such as computed tomography and radiography are essential non-destructive testing (NDT) to visualize the internal geometry of an object. In particular, micro-computed tomography (XCT) is the ideal tool by quantifying the microstructure three-dimensionally in high-resolution [1]. But even three-dimensional non-destructive techniques like XCT are not able to detect defects that are below the physical resolution of the respective system. An important innovation in X-ray technology overcomes this challenge by introducing Talbot-Lau grating interferometer XCT (TLGI-XCT). TLGI-XCT was initially introduced for synchrotron set-ups [2, 3] and subsequently adapted for the use of polychromatic X-ray sources using an additional source grating [4, 5]. This method allows the differentiation of subtle differences in the electron density of two adjacent low absorbing materials [6] and the detection of microscopic density fluctuations in a specimen, e.g. due to micro-pores and micro-cracks, by measuring the effective local small-angle scattering power [7].

TLGI-XCT provides three complementary characteristics in a single scan of the same specimen:

I. attenuation contrast (AC)
II. differential phase contrast / refraction contrast (DPC)
III. dark-field contrast/small angle X-ray scattering contrast (DFC)

AC provides information on the attenuation of the X-ray beam intensity through the specimen and it is thus equivalent to conventional X-ray imaging. DPC is related to the index of refraction and image contrast is thus achieved through the local deflection of the X-ray beam. DFC reflects the total amount of radiation scattered at small angles, e.g. caused by microscopic inhomogeneities in the sample represented by particles, pores, and fibers. In order to generate three-dimensional data, the three complementary sets of AC, DPC, and DFC projections are acquired stepwise at different angles of a full rotation of the specimen, and subsequently reconstructed to volumetric datasets of the absorption, refraction and linear scattering coefficient.

TLGI-XCT has a big potential in the non-destructive testing of FRPs since it provides complementary information to standard AC methods in the form of DPC and DFC images. In particular DFC images reveal information undisclosed by both AC and DPC imaging since DFC delivers morphological information in the sub-pixel regime depending on the local scattering power [7,8]. In addition, dark field images yield a high contrast and a strong signal of interfaces. This improves segmentation and the subsequent quantification of internal defects like micro-cracks and micro-pores [9–11] (see Fig. 1).

In general, the state of the art NDT for porosity detection in carbon fiber reinforced polymers (CFRP) is ultrasonic testing [12] and acid digestion [13], which are not able to deliver a three-dimensional representation of the components internal structure. But even three-dimensional non-destructive techniques like XCT are not able to detect defects that are below the physical resolution of the respective system. In particular, using traditional NDT methods it is not possible to detect and characterize internal cracks and micro-cracks in three-dimensions and their propagation during mechanical testing. In many applications CFRP composite elements are subject to cyclic or intermittent loads which can initiate and promote defects even if initial cracks cannot be detected with non-destructive testing [14, 15]. For designing automotive and aerospace CFRP structures understanding fatigue defect initiation and growth is hence crucial [16].

In this contribution we qualitatively and quantitatively characterize cracks and micro-cracks in the (sub-) micrometer range in CFRP and polymer samples using TLGI-

XCT and compare the results to standard XCT. CFRP samples were subjected to impact tests while polypropylene (PP) test specimens were subject to interrupted fatigue loading. The goal is to detect (micro-) cracks in samples that were subjected to low impact forces or in an early phase of defect initiation respectively.

2. Materials and Methods

2.1 Test samples and mechanical testing

In case 1 we impaired five carbon fiber reinforced laminate plates (20cm x 20cm) using a ball impact test for low impact energies (3 and 5 Joules) and a high-velocity gas gun for impact forces at 10, 15, and 20 Joules. The CFRP laminate were 3 mm in thickness, consisting of 15 layers and had a weight of 311,3g/m² (PREPREG C AGP193-P / 8552S / 38%) respectively. Samples for the TLGI-XCT investigations were cut out of the plates and showed a height of 5 cm and a width of 2 cm.

In case 2, we investigated one polypropylene test specimen that was cyclically loaded in tensile testing until final failure. To guarantee, that the damage will occur in the region of interest, the sample was notched double sided. The test specimen was 5 cm in height and 1 cm in width. It was put under load for 434631 cycles until breakage. The total duration of the procedure was 910 minutes which was performed in four intervals. The load (F_{min}= 55 N and F_{max} = 550 N) was applied at 8 Hz.

2.2 NDT techniques

Specimens were scanned at isometric voxel sizes of 22.8 µm using a Talbot-Lau grating interferometer XCT (Skyscan 1294). This new device was developed by Bruker microCT (www.skyscan.be) on the basis of a small-animal in-vivo phase-contrast micro-XCT scanner [17]. The TLGI-XCT system has a X-ray source with continuously adjustable 20-60 kV peak energy, 100W maximum power and a 33um spot size.

We applied data fusion and image analysis techniques for AC and DFC data for the three-dimensional and multivariate characterization of the materials systems in case 1 (CFRP laminate) and case 2 (PP test specimen) using VGStudioMax 2.2 (Volume Graphics) and Matlab. The isotropic voxel size is 5.7 µm, offering the possibility of binning in 2x2 and 4x4 mode.

For all samples high-resolution reference scans at a voxel size of 5.7 µm and 11 µm were carried out using a sub-XCT system (GE Nanotom x|ray 180NF). Table 1 summarizes the scan parameters for the Talbot-Lau grating interferometer XCT and sub-XCT scans. Talbot-Lau XCT results of case 1 are compared to ultrasonic examinations.

Table 1 Scan parameters: voltage (U) in kV, current (I) in µA, integration time (t_i) in ms, number of projections (N_{proj}), voxel size (VS) in µm, and filter

	U	**I**	**T_i**	**N_{proj}**	**VS**	**filter**
Case 1 (CFRP)						
TLGI-XCT (Skyscan)	35	1100	650	720	22.8	0.25 Al
XCT (Nanotom)	50	490	500	1700	11	-
Case 2 (PP)						
TLGI-XCT (Skyscan)	35	1100	650	720	22.8	0.25 Al
XCT (Nanotom)	55	420	500	1700	5.7	-

3. Results

3.1 CFRP laminates

Figure 1 shows the TLGI- and XCT scans of the 3J sample and Figure 2 shows a comparison of AC and DFC images in the 3J and 5J sample. Voxel size (VS) for the XCT scan is 11 µm, VS for the DFC images is 22.8 µm.

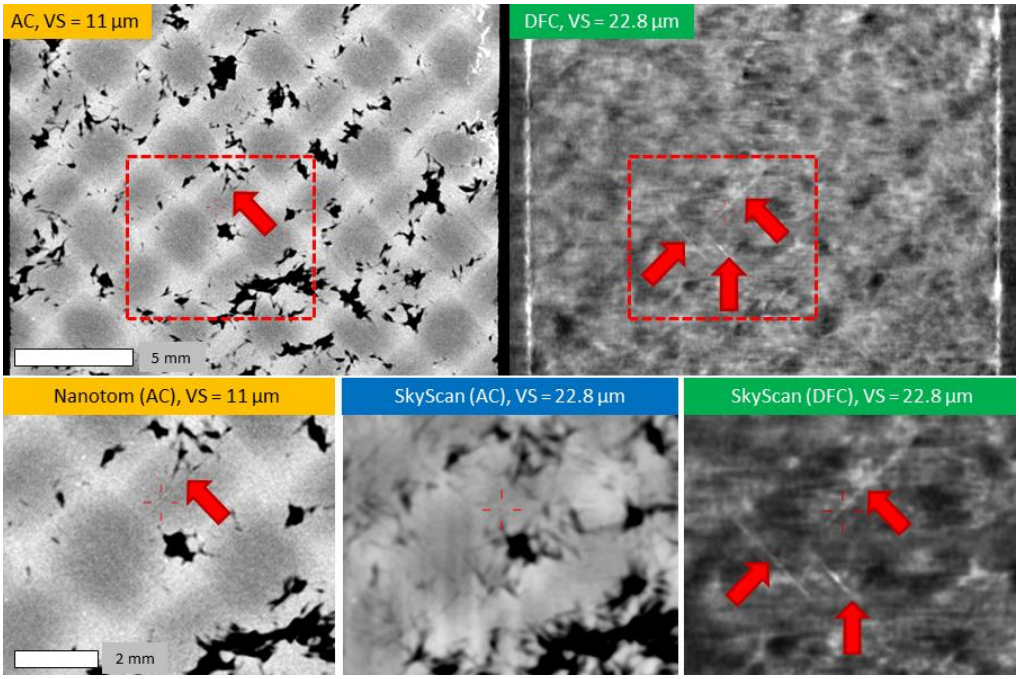

Fig. 1 Front view slices of CFRP impact sample (3J). Upper left: Sample overview at the side opposite of the impact site using standard XCT (VS: 11 µm). Upper right: DFC overview. Bottom row: AC detailed view (VS: 11 µm, left), AC detailed view (VS: 22.8 µm, middle), DFC detailed view (VS: 22.8 µm, middle); red arrows indicate micro-cracks in the same slice respectively.

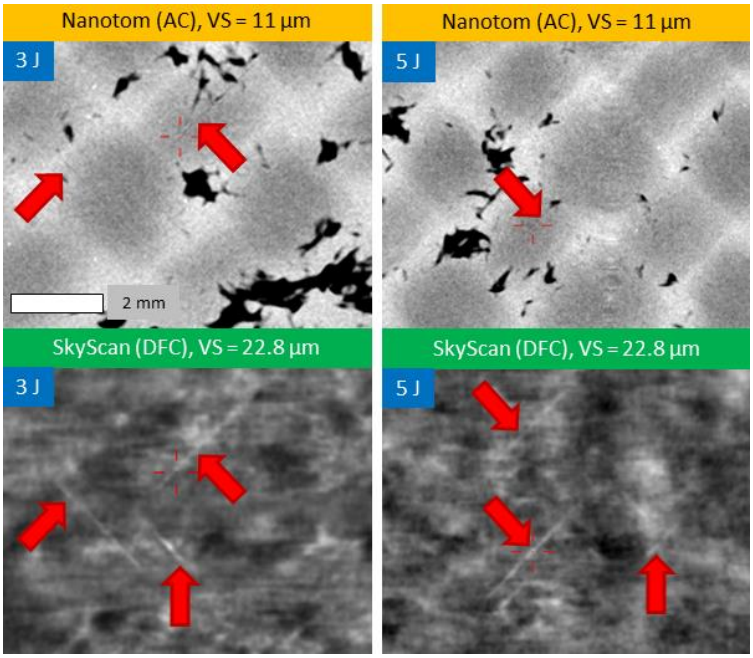

Fig. 2 CFRP laminates impaired during impact damages at 3J (left) and 5J (right). Upper row: Standard XCT images (VS: 11 µm). Bottom row: DFC images (VS: 22.8 µm); red arrows indicate the sites of micro-cracks.

Even though the voxel size is twice as high in the DFC images, micro-cracks can be detected in the DFC volume data. In contrast, micro-cracks are hardly visible in AC images (see red arrows in Fig. 1 and Fig. 2).

For the sample with higher impact energy (10 J) cracks were extensive and clearly visible using standard XCT at the opposite side of the impact. Nevertheless, Figure 3 shows that cracks cannot be detected at the impact site in the case of AC images, whereas the DFC signal at the impact location clearly shows defects. We compared AC and DFC images to results of ultrasonic testing, showing the position along the thickness and extension of delaminations in the CFRP subjected to an impact test (10J).

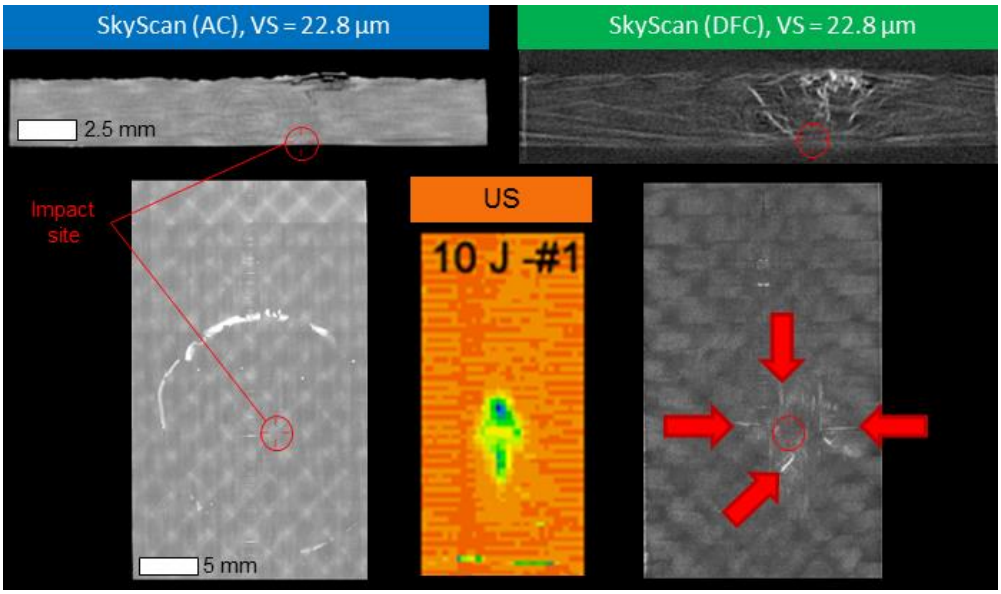

Fig. 3 CFRP laminate subjected to impact damage at 10J. Impact location depicted by red circle Upper row: Transversal slices (VS: 11 µm). Frontal images at the site of impact (bottom row): AC image (left), ultrasonic evaluation (middle), and DFC image right)

We quantified the amount of defects detectable in AC and DFC images (see Fig. 4 for DFC at 10J to 20J). Maximum defect depth (in millimeter) was defined as a visually detectable crack in the volume of the same sample. We manually estimated maximum defect depth for the 5J, 10J, 15J, and 20J samples (Fig. 4, right) and showed that, in contrast to AC images defects can be detected in the whole axial plane using DFC imaging.

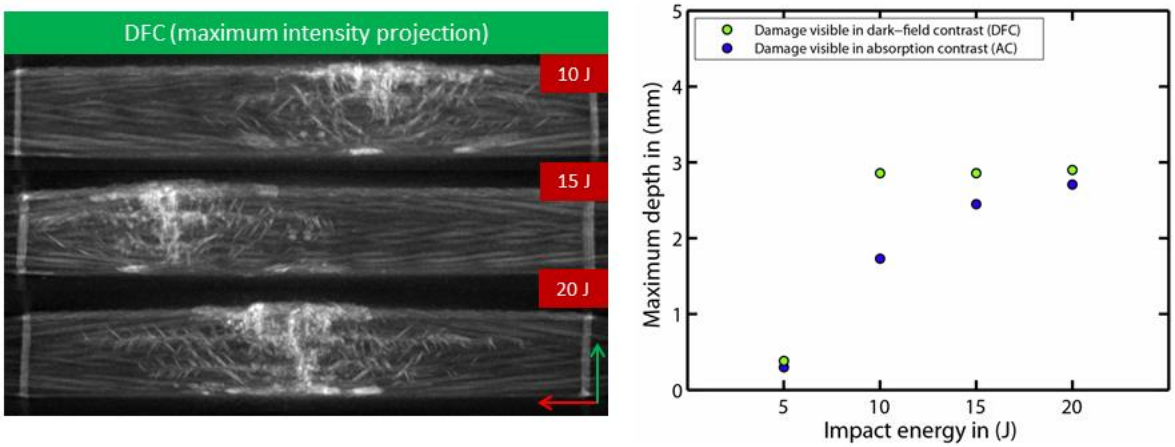

Fig. 4 CFRP laminates subjected to impact damage. Left: In DFC images cracks can be detected in the whole volume of the axial plane for 10J, 15J, and 20J samples. Right: Comparison between estimated defect depth in the axial plane between AC (blue circles) and DFC (green circles) images.

3.2 Polypropylene test specimen

In case 2 we investigated a PP specimen that was cyclically loaded in interrupted tensile testing until final failure. In total, the test specimen was loaded in four intervals. The first and second interval involved 172000 cycles respectively (time range: 0 – 360 min and 360 – 720 min respectively), the third interval comprised 86000 cycles (720 – 900 min). The sample broke after 4631 cycles in the last interval (900 – 910 min). Figure 4 shows AC and DFC images of the PP specimen in the original, unaffected state (Fig. 4a and b), after the first interval (Fig. 4c and d), after the second interval (Fig. 4e and f) and after the third interval (Fig. 4g and h).

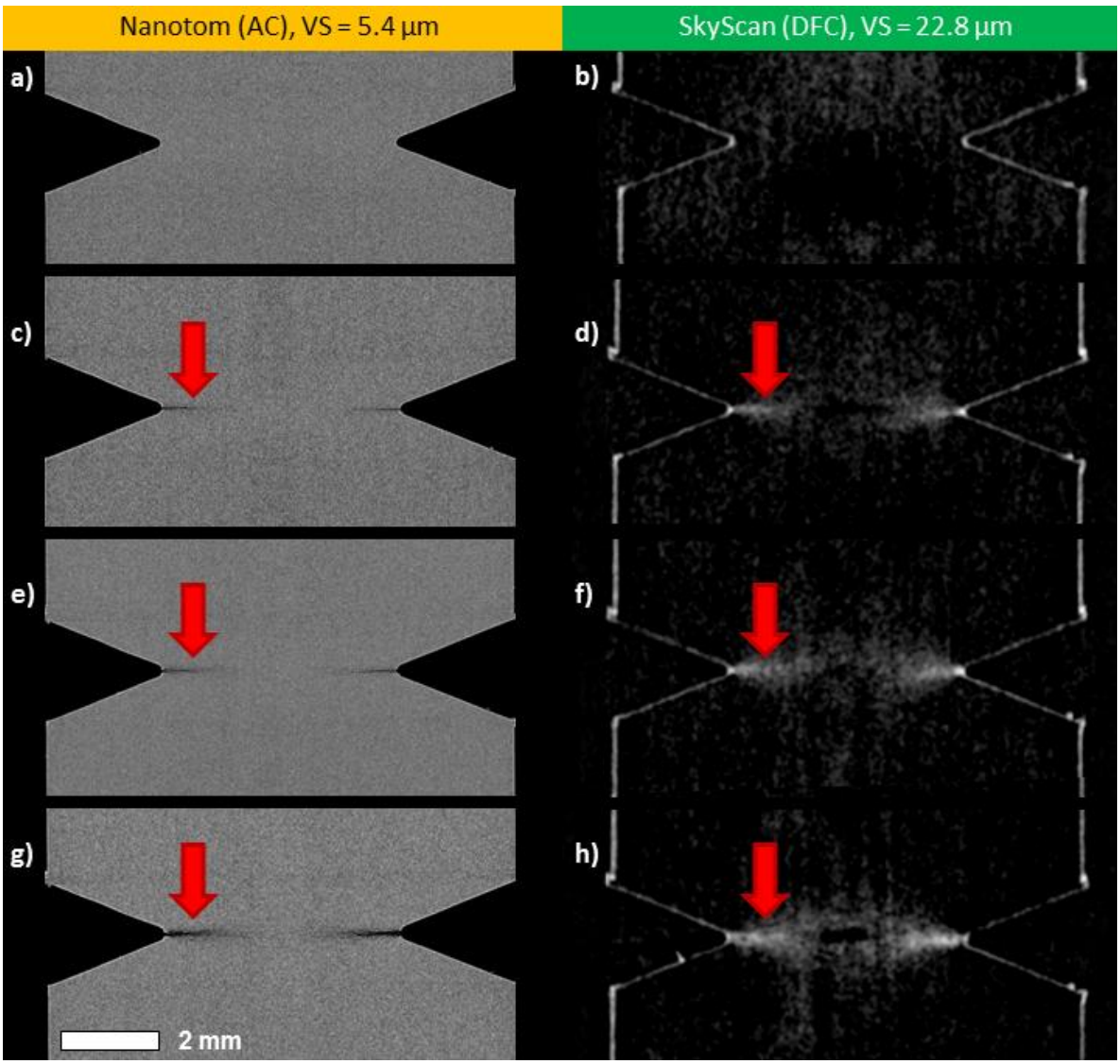

Fig. 5 Frontal AC (left row) and DFC (right row) images of a PP test specimen subjected to interrupted cycling loading. Initial state: a) and b), after 172000 cycles: c) and d), after 344000 cycles: e) and f), and after 430000 cycles: g) and h). Red arrows indicate accumulations of defects in the notch region during loading.

After the first loading interval, appearing cracks are obvious in the AC image represented by lower grey levels in the notch region. Those defects propagate during the subsequent intervals showing extensive accumulations of defects after the third interval. Accordingly, the dark field signal intensity increases during the different stages, showing a spindle-shaped region in the second last interval (Fig. 4h).

4. Discussion and conclusions

Talbot-Lau grating interferometer XCT (TLGI-XCT) is a new innovative X-ray technology that expands imaging possibilities of standard XCT in material science by delivering information in form of dark-field contrast (DFC). Even though XCT imaging is a powerful tool for three-dimensional materials characterization, conventional absorption-based methods are not able to detect defects that are below the physical resolution of the respective system. The introduction of DFC imaging helps to overcome this limitation.

We showed that DFC allows the identification of cracks in CFRP laminates, which are smaller than the spatial resolution of the reference XCT system. Sample size is a major limiting factor in high-resolution XCT, however DFC imaging allows the identification of (micro-) cracks in relatively large samples with at a relatively low spatial resolution, in our case at 22.8 µm (see Fig. 1 and 2). In contrast to the reference XCT scan at 11 µm, even small cracks at the opposite site of the impact location could be detected using TLGI-XCT (see Fig. 3). Moreover, we were able to show that the amount of defect detectable in DFC images exceeded the information on defect distribution in AC images, in particular for the 10J sample (see Fig. 4). A systematic investigation using multiple samples that will be subjected to different impact forces is needed to rigorously evaluate the relationship between defect detectability in AC and DFC in various combinations of sample properties (thickness, weave pattern, matrix etc.) and impact forces.

In general, there are certain limitations in relation to TLGI-XCT that have to be considered prior to a more comprehensive use of DFC imaging for materials characterization and defect detection. Primarily, there are only few investigations of DFC imaging for sub-pixel crack detection [9, 18]. Basically, studies on the relationship between dark field signal intensity and actual crack width, e.g. using reference methods like XCT or scanning electron microscopy, are lacking. A first step to overcome this shortcoming was the investigation of a PP test specimen that was subjected to interrupted cyclic loading experiments. Scans between the loading intervals with XCT and TLGI-XCT showed a correspondence between the AC and DFC signals (see Fig. 5). Further studies using DFC phantoms have to evaluate the underlying relationships between DFC signal and amount and distribution of internal microscopic inhomogeneities like cracks and pores.

Acknowledgments

The work was financed by the K-Project ZPT+, supported by the COMET programme of FFG and by the federal government of Upper Austria and Styria.

References

[1] Kastner J (Editor). Conference on Industrial Computed Tomography. Wels, Austria: Shaker; 2014.

[2] David C, Nöhammer B, Solak HH, Ziegler E. Differential x-ray phase contrast imaging using a shearing interferometer. Appl Phys Lett 2002;81:3287.

[3] Momose A, Kawamoto S, Koyama I, Hamaishi Y, Takai K, Suzuki Y. Demonstration of X-Ray Talbot Interferometry. Jpn J Appl Phys 2003;42:L866–8.

[4] Pfeiffer F, Weitkamp T, Bunk O, David C. Phase retrieval and differential phase-contrast imaging with low-brilliance X-ray sources. Nat Phys 2006;2:258–61.

[5] Pfeiffer F, Bech M, Bunk O, Kraft P, Eikenberry EF, Brönnimann C, et al. Hard-X-ray dark-field imaging using a grating interferometer. Nat Mater 2008;7:134–7.

[6] Stampanoni M, Wang Z, Thüring T, David C, Rössl E, Stevendaal U Van, et al. Toward clinical differential phase contrast mammography: preliminary evaluations and image processing schemes. J Instrum 2013;8:C05009–C05009.

[7] Bech M, Bunk O, Donath T, Feidenhans'l R, David C, Pfeiffer F. Quantitative x-ray dark-field computed tomography. Phys Med Biol 2010;55:5529–39.

[8] Kastner J, Senck S, Gusenbauera C, Plank B, Heinzl C, Sasov A. Three-dimensional characterization of fibre-reinforced polymers using a Talbot-Lau grating interferometer µ-CT and data fusion methods. XNPIG, 2015, p. 32–3.

[9] Lauridsen T, Willner M, Bech M, Pfeiffer F, Feidenhans'l R. Detection of sub-pixel fractures in X-ray dark-field tomography. Appl Phys A 2015:1–8.

[10] Revol V, Jerjen I, Kottler C, Schütz P, Kaufmann R, Lüthi T, et al. Sub-pixel porosity revealed by x-ray scatter dark field imaging. J Appl Phys 2011;110:044912.

[11] Revol V, Plank B, Kaufmann R, Kastner J, Kottler C, Neels A. Laminate fibre structure characterisation of carbon fibre-reinforced polymers by X-ray scatter dark field imaging with a grating interferometer. NDT E Int 2013;58:64–71.

[12] Birt; EA, RA S. A review of NDE methods for porosity measurement in fibre-reinforced polymer composites. Insight 2004;46:681–6.

[13] DIN. EN 2564: Aerospace series - carbon fibre laminates - determination of the fibre-, resin- and void contents 1998:1–12.

[14] Stelzer S, Jones R, Brunner A. Interlaminar fatigue crack growth in carbon fiber reinforced composites. Conf Compos 2013:1–9.

[15] Carvelli V, Feo L, Pegoretti A, Quaresimin M, Zappalorto M. Advances in damage mechanics of polymer composites. Compos Part B Eng 2014;65:1.

[16] Martin RH. Incorporating interlaminar fracture mechanics into design. Proc. Inst. Mech. Eng. Part L J. Mater. Des. Appl., 2000, p. 91–7.

[17] Pauwels B, Bruyndonckx P, Liu X, Tapfer A, Velroyen A, Yaroshenko A, et al. First small-animal in-vivo phase-contrast micro-CT scanner. SPIE 8506, Dev X-Ray Tomogr VIII 2012.

[18] Gusenbauer C, Leiss-Holzinger E, Senck S, Mathmann K, Kastner J, Hunger S, et al. Characterization of medical and biological samples with a Talbot–Lau grating interferometer µXCT in comparison to reference methods. Case Stud Nondestruct Test Eval 2016;1:1–9.